Acta Physiologica Sinica, August 25, 2008, 60 (4): 525-534
http://www.actaps.com.cn

Research Paper

Blockade of the human *ether-a-go-go*-related gene potassium channel by ketanserin

TU Dan-Na, ZOU An-Ruo, LIAO Yu-Hua*, DU Yi-Mei, WANG Xian-Pei, LI Lu

Research Center of Ion Channelopathy, Department of Cardiology, Institute of Cardiovascular Diseases, Union Hospital, Tongji Medical College, Huazhong University of Science and Technology, Wuhan 430022, China

Abstract: In the present study, we investigated the inhibitory action of ketanserin on wild-type (WT) and Y652 mutant human *ether-a-go-go*-related gene (HERG) potassium channels expressed in *Xenopus* oocytes and the effects of changing the channel molecular determinants characteristics on the blockade with and without ketanserin intervention using standard two-microelectrode voltage-clamp techniques. Point mutations were introduced into HERG gene (Y652A and Y652R) and subcloned into the pSP64 plasmid expression vector. Complementary RNAs for injection into oocytes were prepared with SP6 Cap-Scribe after linearization of the expression construct with *EcoR* I. Clampfit 9.2 software was employed for data collection and analysis. Origin 6.0 software was used to fit the data, calculate time constants and plot histograms. The results showed that ketanserin blocked WT HERG currents in voltage- and concentration-dependent manner and showed minimal tonic blockade of HERG current evaluated by the envelope of tails test. The IC_{50} value was (0.38±0.04) μmol/L for WT HERG potassium channel. The peaks of the *I-V* relationship for HERG channel suggested a negative shift in the voltage-dependence of activation after using ketanserin, whose midpoint of activation values ($V_{1/2}$) were (-16.59±1.01) mV (control) *vs* (-20.59±0.87) mV (ketanserin) at 0.1 μmol/L, (-22.39±0.94) mV at 1 μmol/L, (-23.51±0.91) mV at 10 μmol/L, respectively (P<0.05, n=6). Characteristics of blockade were consistent with an open-state channel blockade, because the extent and rate of onset of blockade was voltage-dependent, increasing at more potentials even in the condition of leftward shift of activation curve. Meanwhile, in the different depolarization duration, the fractional blockade of end-pulse step current and peak tail current at 100 ms duration was significantly lower than that at 400 ms and 700 ms, which indicated that following the channel activation fractional blockade was enhanced by the activated channels. Ketanserin could also modulate the inactivation of HERG channel, which shifted the voltage-dependence of WT HERG channel inactivation curve from (-51.71±2.15) mV to (-80.76±14.98) mV (P<0.05, n=4). The S6 mutation, Y652A and Y652R, significantly attenuated the blockade by ketanserin. The IC_{50} value were (27.13±9.40) μmol/L and (20.20±2.80) μmol/L, respectively, increased by approximately 72-fold for Y652A and 53-fold for Y652R compared to that of WT HERG channel blockade [(0.38±0.04) μmol/L]. However, between the inhibitory effects of Y652A and Y652R, there was no significant difference. In conclusion, ketanserin blocks WT HERG currents in voltage- and concentration-dependent manner and preferentially blocks open-state HERG channels. Tyr-652 is one of the critical residues in the ketanserin-binding sites.

Key words: human *ether-a-go-go*-related gene; potassium channels; ketanserin; voltage-clamp techniques; mutation

酮色林对人类 *ether-a-go-go* 相关基因钾通道的阻断作用

涂丹娜，邹安若，廖玉华*，杜以梅，王宪沛，李璐

华中科技大学同济医学院附属协和医院心血管病研究所，心内科，离子通道病研究中心，武汉 430022

摘 要：采用双电极电压钳技术，研究酮色林对表达在非洲爪蟾卵母细胞上的野生型和 Y652 突变型人类 *ether-a-go-go* 相关基因(human *ether-a-go-go*-related gene, HERG)钾通道的阻断效应，观测 HERG 通道的分子位点特性改变对其阻断效应的影响。结果显示，酮色林以电压依赖性和浓度依赖性的方式阻断野生型的 HERG 钾通道电流。尾电流包裹程序记录电流显示酮色林对 HERG 钾通道微小的张力性阻断。阻断特征符合对开放状态通道的阻断特征。酮色林也能调节失活状态的 HERG 钾通道。位

Received 2008-03-03 Accepted 2008-05-06

This work was supported by the National Natural Science Foundation of China (No. 30470711).

*Corresponding author. Tel: +86-27-85726462; Fax: +86-27-85727340; E-mail: liaoyh27@163.com

于孔道 S6 区的氨基酸位点突变 Y652A 和 Y652R 可显著减弱酮色林对 HERG 通道的阻断作用。同野生型 HERG 钾通道的阻断相比，Y652A 突变使阻断的 IC_{50} 提高 72 倍，而 Y652R 突变使阻断的 IC_{50} 提高 53 倍。Y652A 和 Y652R 的阻断效应之间没有明显的差别。以上结果提示，酮色林优先阻断开放状态的 HERG 钾通道，而 Y652 是酮色林与通道结合的关键位点之一。

关键词：人类 *ether-a-go-go* 相关基因；钾通道；酮色林；电压钳技术；突变
中图分类号：Q25

The human *ether-a-go-go*-related gene (HERG)[1] encodes the pore-forming α-subunits of channels that conduct the rapid delayed rectifier K^+ current (I_{kr})[2], which is one of the most important membrane currents responsible for ventricular action potential repolarization. The suppression of HERG channels can lead to electrophysiological and electrocardiographic changes including action potential duration (APD) and QT interval prolongation, which can both be antiarrhythmic and cause long-QT syndrome (LQTS)[3]. More commonly, LQTS is an adverse effect of many different types of drugs, including antiarrhythmics, antihistamines, antibiotics, gastrointestinal prokinetics, and antipsychotics[4,5]. It has been documented that diverse structure drugs-induced QT prolongation is mainly due to the drug-mediated inhibition of I_{kr} [4-7]. Structure function data provides evidence that the pore cavity of HERG channel is larger than that of other voltage-gated K^+ (Kv) channels. Moreover, the aromatic amino acids that present in the inner (S6) helices of HERG are absent from Kv channels, which form key components of a high-affinity drug binding site. These features appear to confer upon the HERG channel a unique susceptibility to pharmacological blockade[8].

Because of their potential pro-arrhythmic effects, a number of non-cardiac drugs have been withdrawn from the market (e.g. terfenadine, cisapride and thioridazine) and many have been labeled for restricted use (e.g. mesoridazine, droperidol and arsenic trioxide). Therefore, screening compounds for HERG and QT interval liability is now a routine in the pharmaceutical industry. To facilitate the rational design of safer drugs without HERG liability, it is important to understand the biophysical and molecular mechanisms of HERG channel blocked by drugs. Ketanserin is a selective serotonin (5-HT) 2 receptor antagonist with minor α1-receptor and 5-HT1 receptor blocking properties. It reduced peripheral blood pressure through blocking the activating role of peripheral 5-HT on 5-HT receptor and has been evaluated for the treatment of hypertension, especially the treatment of severe hypertension in pregnancy, and certain peripheral vascular disease[9]. Furthermore, ketanserin has been suggested to diminish arteriosclerotic development by its effect on serotonin-induced platelet aggregation and thrombus formation[10]. However, previous reports showed that QT intervals of some patients using ketanserin therapy were prolonged[11,12]. And some studies verified that ketanserin, similar to other drugs, could inhibit I_{kr} in guinea pig myocardial cell, and induce QT interval prolongation[12]. So far, complete biophysical properties and molecular determinants for ketanserin blocking HERG channel have not been reported. In the present study, therefore, we investigated the effect of ketanserin on wild-type (WT) and mutant HERG channels expressed in *Xenopus* oocytes and observed the properties and the molecular basis of the ketanserin blocking the HERG channels.

1 MATERIALS AND METHODS

1.1 *Molecular biology*

Point mutations were introduced into HERG gene (Y652A and Y652R) and subcloned into the pSP64 plasmid expression vector (Promega, Madison, WI), which was a gift from Professor Michael C. Sanguinetti of University of Utah. Before being used in experiments, each construct was confirmed with restriction mapping and DNA sequencing of the PCR-amplified segment. Complementary RNAs (cRNAs) for injection into oocytes were prepared with SP6 Cap-Scribe (Roche Molecular Biochemicals) after linearization of the expression construct with *EcoR* I.

1.2 *Isolation and injection of oocytes*

Xenopus frogs were anesthetized by immersion in 0.2% tricaine for 15-30 min. Ovarian lobes were digested with 1.5 mg/mL type 1A collagenease (Sigma) in Ca^{2+}-free ND96 solution for 1 h to remove follicle cells. Stage IV and V *Xenopus laevis* oocytes were injected with 46 nL of HERG cRNAs and then cultured in ND96 solution supplemented with 100 U/mL penicillin, 100 U/mL streptomycin and 2.5 mmol/L pyruvate at 18 °C for 1-3 d before being used in voltage clamp experiments. ND96 solution contained (in mmol/L) NaCl 96, KCl 2, $CaCl_2$ 1.8, $MgCl_2$ 2, HEPES 5, and the pH was adjusted to 7.6 with NaOH.

1.3 *Two-microelectrode voltage clamp of oocytes*

A TEV-200 amplifier (Dagan Corporation) and standard

two-microelectrode voltage clamp techniques were used to record currents. Currents were recorded at room temperature (22-24 °C) 2-10 d after cRNA injection. Glass microelectrodes were filled with 3 mol/L KCl, and their tips were broken to obtain resistances of 1-3 MΩ. pCLAMP software (version 9.2; Molecular Devices, Union City, CA) and a 1322A interface (Molecular Devices, Union City, CA) were used to generate voltage commands. Currents were digitally sampled at 5 kHz and filtered at 2 kHz. Leak and capacitive currents were not corrected. The oocytes were superfused with ND96 solution at a rate of 1 mL/min, and the membrane potential was held at -80 mV between test pulses, which were applied at a rate of 1-3 /min. Currents were measured before and 10 min after drug application to the bath.

1.4 *Drugs*

Ketanserin (Sigma, USA) was prepared as 10 mmol/L stock solution. Before the experiments, the stock solution was diluted with external solution to reach the desired final concentration. Oocytes were exposed to ketanserin solutions until steady state effects were achieved, usually for about 15 min.

1.5 *Data analysis*

Clampfit 9.2 software was employed for data collection and analysis. Origin 6.0 software (nonlinear curve fitting) was used to fit the data, calculate time constants and plot histograms. Fractional blockade was defined as follows: $f=1-I_{drug}/I_{control}$, where $I_{control}$ and I_{drug} are the current amplitudes in the absence and presence of ketanserin, respectively. Dose-response curves were fit by the Hill equation: $(I_{control}-I_{drug})/I_{control}=B_{max}/[1+(IC_{50}/D)^n]$, where B_{max} is the maximum blockade of currents; IC_{50} is the concentration of ketanserin for half-maximum blockade; D is the concentration of ketanserin, and n is the Hill coefficient. The activation curve was approximated by the normalized conductance-voltage relationship and fitted with a Boltzmann function: $y=A/\{1+\exp[(V_{1/2}-Vm)/k]\}$, where A is the amplitude term, $V_{1/2}$ is the midpoint of activation, Vm is the test potential, and k represents the slope factor of the curve. The curve-fitting procedure used a nonlinear least-squares (Gauss-Newton) algorithm; results were displayed in linear and semilogarithmic format, together with the difference plot. Goodness of fit was judged by the χ^2 criterion and by inspection for systematic nonrandom trends in the difference plot. Data were presented as means±SEM. Student's *t* tests for paired and unpaired data were used to compare the control group with the treated group. A value of $P<0.05$ was considered to be statistically significant.

2 RESULTS

2.1 Identification of pSP64-HERG plasmid vector and HERG currents

pSP64-HERG plasmid vector was 6.497 kbp long. While using *EcoR* I or *Hind* III restriction enzyme to digest it, the length of linear fragment was consistent with above mentioned (Fig. 1*A*). While using *EcoR* I and *Hind* III restriction enzyme together to digest it, we got two fragments of 3.551 kbp and 2.946 kbp (Fig. 1*A*), respectively. These results showed that the plasmid extracted from DH-5α colibacillus was target plasmid. Membrane potential was held at -80 mV, currents were elicited by 2-s depolarizing pulses to potentials ranging from -60 to +60 mV, and the tail currents measured on return to -50 mV. Specific blocking agent of HERG channel E-4031 was used to identify whether the recorded currents were HERG currents or not[13]. Figure 1*B* showed the original current traces before and after incubation with 3 μmol/L E-4031. The currents were blocked markedly, indicating that the recorded currents are HERG currents.

2.2 Concentration- and voltage-dependent blockade of WT HERG channel by ketanserin in *Xenopus* oocytes

Currents were elicited by 2-s depolarizing pulses to potentials ranging from -60 to +60 mV from a holding potential at -80 mV. An example of WT HERG currents recorded before and after addition of 1 μmol/L ketanserin was shown in Fig. 2*A* and 2*B*. The normalized *I-V* relationship of WT HERG channel for step currents measured at the end of 2-s pulses (Fig. 2*C*) and the tail currents measured on return to -50 mV (Fig. 2*D*) were reduced by ketanserin in a concentration-dependent manner. The value of IC_{50} is (0.38±0.04) μmol/L (n=6) at 0 mV. Blockade was also voltage-dependent. At the more negative test potential, ketanserin exerted comparatively little effect on HERG current, and even in some experiments, the tail current magnitude was greater in the presence of ketanserin than that in control solution. At test potentials more positive than -40 mV, a marked inhibitory effect was observed in all cells on step current and peak tail current. Furthermore, greater blockade happened apparently at more depolarized potentials (Fig. 2*C*, 2*D*). Figure 2*E* showed the fractional blockade of step currents and tail currents of HERG channel at different test potentials. At voltage ranging from -40 to +40 mV, the fractional blockade of the tail currents gradually

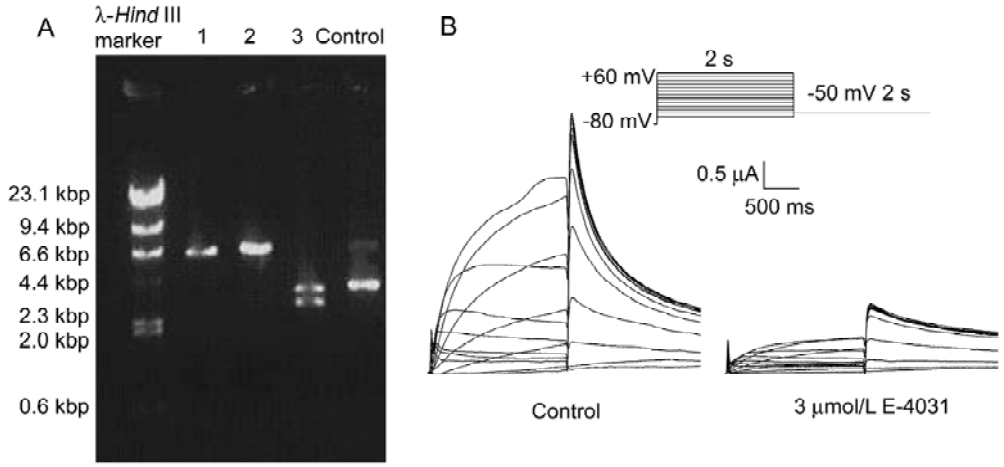

Fig. 1. Identification of pSP64-HERG plasmid vector and HERG currents. *A*: Electrophoresis identification of pSP64-HERG plasmid vector. Lane 1, plasmid with *EcoR* I restriction enzyme digestion; Lane 2, plasmid with *Hind* III restriction enzyme digestion; Lane 3, plasmid with *EcoR* I and *Hind* III restriction enzyme digestion; Control, pSP64-HERG plasmid vector. *B*: Identification of HERG currents. HERG currents were recorded from oocytes before and after incubation with 3 μmol/L E-4031. Currents were recorded at test potentials between -60 and +60 mV. Tail currents were recorded after repolarization to -50 mV.

increased and reached a steady state at +20 mV, However, the fractional blockade of the 2-s end pulse currents firstly increased step by step from -40 mV to +10 mV, then a gradually decrease followed (Fig. 2*E*). The difference of blockade may be attributed to different gating mechanism. If ketanserin preferentially blocks open state HERG channel, rapid inactivation of channel can prevent drug from arriving at binding site with channel or reduce the affinity between drug and channel. However, repolarization removes the inactivation state of channel and abolishes low-affinity binding of drug to channel. In addition, the peaks of the *I-V* relationship for HERG channel were shifted to the left after using ketanserin, suggesting a negative shift in the voltage-dependent activation. This was confirmed by tail current analysis (Fig. 2*F*). For WT HERG channels, the $V_{1/2}$ was (-16.59±1.01) mV in control, (-20.59±0.87) mV at 0.1 μmol/L ketanserin, (-22.39±0.94) mV at 1 μmol/L ketanserin, (-23.51±0.91) mV at 10 μmol/L ketanserin (P<0.05, n=6), and the k was (13.12±0.92) mV in control, (10.71±0.76) mV at 0.1 μmol/L ketanserin, (10.94±0.81) mV at 1 μmol/L ketanserin and (11.00± 0.77) mV at 10 μmol/L ketanserin, respectively (P>0.05, n=6). Thus the dual effect of ketanserin on HERG tail current may be explained by the drug both inhibiting HERG currents and producing a leftward shift in voltage-dependent activation of the channel.

2.3 Time-dependent blockade of WT HERG channel by ketanserin in *Xenopus* oocytes

The time course of the development of HERG channel blockade by ketanserin was investigated using an 'envelope of tails' protocol[14,15]. Membrane potential was held at -80 mV and stepped to +40 mV for increasing durations between 20 and 700 ms, after which HERG tails were evoked on repolarization to -40 mV. Original current traces before and after addition of 1 μmol/L ketanserin were shown in Fig. 3*A* and 3*B*. The time-dependence of evoked tail activation was fitted with a monoexponential equation, for WT HERG channels, yielding a τ of (84.87±3.10) ms for control and (52.79±3.37) ms for ketanserin (n=4, P< 0.05, Fig. 3*C*). The fractional blockade of the tail currents was plotted with each time duration by monoexponential equation, for WT HERG channels, yielding a τ of (123.61± 4.42) ms for the onset of post-depolarization channel blockade by 1 μmol/L ketanserin (Fig. 3*D*). Figure 3*E* showed that 1 μmol/L ketanserin produced an attenuation of HERG current after a 100 ms activating pulse. The levels of inhibition of step currents and tail currents were enhanced with 400 ms and 700 ms duration command pulses compared with the blockade level of those with 100 ms duration (n=4, P<0.05, Fig. 3*F*). While between the fractional blockade in 400 ms and 700 ms duration depolarization, there was no significant difference (n=4, Fig. 3*F*). These data indicated that the blockade was enhanced by further activation of the channel, which is concordant with the fact that the drug can block the open-state channel.

2.4 Effect of ketanserin on inactivation of WT HERG channels in *Xenopus* oocytes

After a 2-s pulse to +40 mV, the membrane potential was

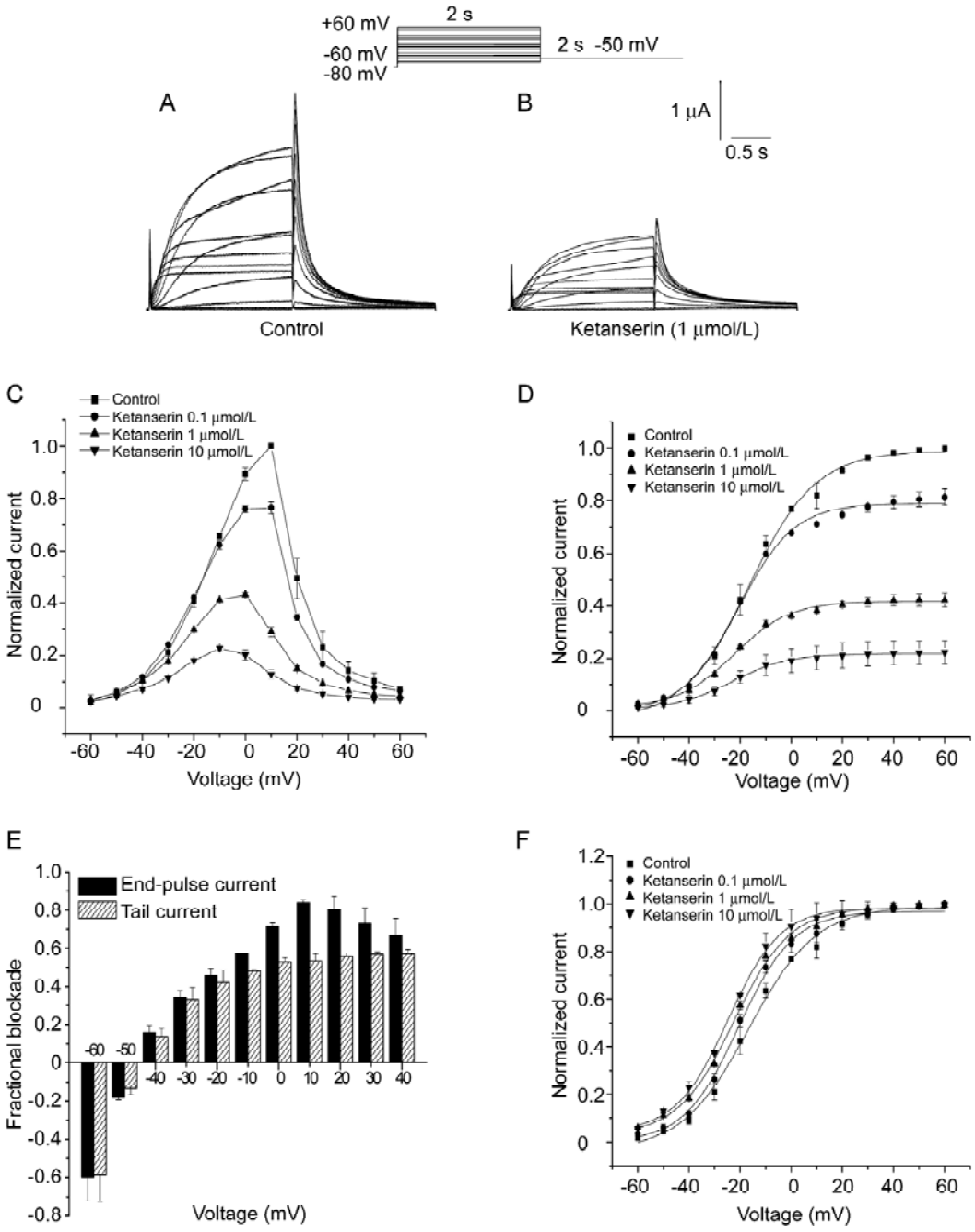

Fig. 2. Effect of ketanserin on wild-type HERG channel activation in *Xenopus* oocytes. *A* and *B*: Representative HERG currents recorded from an oocyte before (*A*) and after (*B*) incubation with 1 μmol/L ketanserin. Currents were recorded at test potentials between -60 and +60 mV. Tail currents were recorded after repolarization to -50 mV. *C*: *I-V* curves for currents measured at the end of the 2-s test pulse with and without application of 0.1, 1 and 10 μmol/L ketanserin (n=6). Currents were normalized to the control current at 0 mV for each oocyte. *D*: *I-V* curves for peak tail currents with and without application of 0.1, 1 and 10 μmol/L ketanserin (n=6). Currents were normalized to the peak current measured in the control condition for each oocyte. *E*: Mean data of the voltage-dependent fractional blockade, defined as the amplitude of current reduced by drug divided by control current amplitude ($1-I_{drug}/I_{control}$), of HERG tail (filled bars) and end-pulse currents (bias bars). *F*: Effect of ketanserin on the isochronal activation curves for HERG. Tail currents were normalized to the peak current under each condition, and the data were fit with a Boltzmann function $y = A/\{1 + \exp[(V_{1/2} - V\text{m})/k]\}$. The $V_{1/2}$, respectively, were as following: control: (-16.59±1.01) mV; 0.1 μmol/L ketanserin: (-20.59±0.87) mV; 1 μmol/L ketanserin: (-22.39±0.94) mV; and 10 μmol/L ketanserin: (-23.51±0.91) mV (P<0.05, n=6), however, k, respectively, were as following: control: (13.12±0.92) mV; 0.1 μmol/L ketanserin: (10.71±0.76) mV; 1 μmol/L ketanserin: (10.94±0.81) mV; and 10 μmol/L ketanserin: (11.00±0.77) mV (P>0.05, n=6).

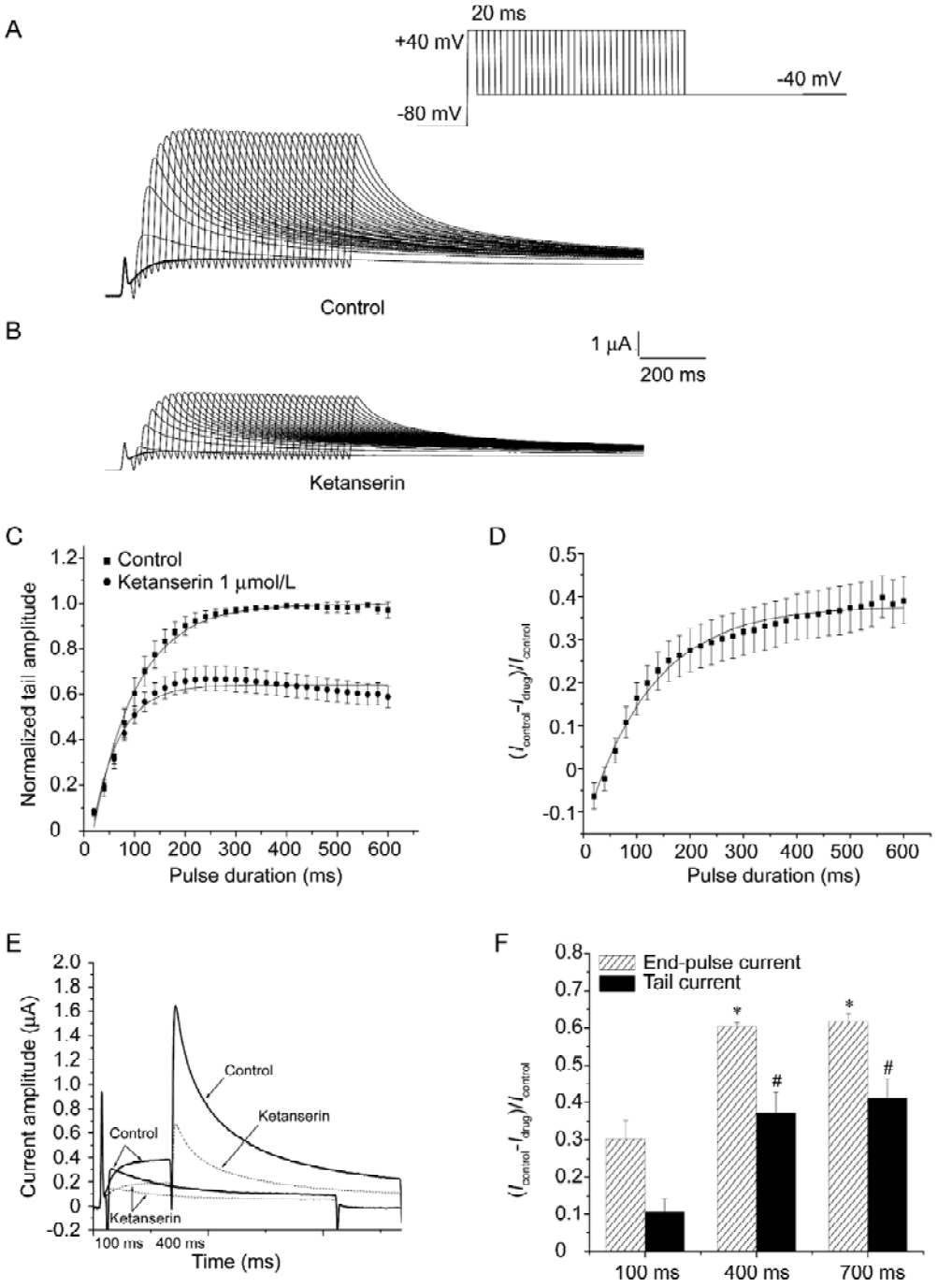

Fig. 3. Time- and state-dependence of wild-type HERG channel blockade by ketanserin. *A* and *B*: Representative current traces evoked by an envelope of tails protocol in the same cell under control condition (*A*) and in the presence of 1 μmol/L ketanserin (*B*). Cells were held at -80 mV and stepped to +40 mV for 20-700 ms in 20 ms interval and then tail currents were evoked on repolarization to -40 mV. Peak tail currents at each time point were measured. *C*: Peak tail current after return to -40 mV was plotted as a function of test pulse duration. Continuous lines represent monoexponential that fits experimental data, yielding a τ of (84.87±3.10) ms for control and (52.79±3.37) ms for ketanserin (n=4, P<0.05). *D*: Fractional tail-current blockade produced by ketanserin as a function of test pulse duration. Continuous line represents monoexponential that fits experimental data with a τ of (123.61±4.42) ms (n=4). *E*: Representative HERG current recorded with 100 and 400 ms depolarization duration before and after addition of 1 μmol/L ketanserin. Membrane potential was held at -80 mV, and then briefly stepped to +40 mV for 100 and 400 ms, respectively, prior to repolarization to -40 mV to elicit HERG tail current. *F*: Fractional blockade of HERG end-pulse step currents and peak tail currents evoked at 100, 400 and 700 ms was summarized. 1 μmol/L ketanserin produced significant greater blockade at 400 and 700 ms duration than that at 100 ms ($^{*}P$<0.05 *vs* end-pulse current at 100 ms duration, n=4; $^{\#}P$<0.05 *vs* tail current at 100 ms duration, n=4). While between the fractional blockade in 400 ms and 700 ms duration depolarization, there was no significant difference (n=4).

held to various test voltages from -120 mV to +40 mV for 20 ms to allow inactivation to relax to a steady-state, and then followed by a return step to +40 mV. Peak current elicited by the second step to +40 mV provided a relative number of open conducting channels, while the re-inactivation of HERG channel was rapid at +40 mV pulse and partially obscured by the capacity transient (Fig. 4*A*). Therefore, peak outward current during the third pulse was estimated by fitting current traces beginning 3 ms after depolarization with a monoexponential equation, and extrapolating to the beginning of the pulse. Then peak current amplitudes were normalized to that of control current at -120 mV and then plotted as a function of the voltage of the 20 ms test pulse (steady-state inactivation curve) and fitted to a Boltzmann function (Fig. 4*B*). Peak current amplitudes were prominently decreased by ketanserin (10 μmol/L). And ketanserin shifted the voltage-dependent WT HERG channel inactivation curve from (-51.71±2.15) mV to (-80.76±14.98) mV ($P<0.05$, $n=4$), indicating that the voltage-dependence of steady-state inactivation of HERG channels can be also modified by ketanserin. However, slope factors [(31.21±2.57) mV *vs* (28.82±9.69) mV)] for the steady-state inactivation were not significantly altered by ketanserin ($n=4$).

2.5 Ketanserin blocks WT and Y652 mutant HERG channels in *Xenopus* oocytes

Previous studies have shown that aromatic residue Tyr-652 located in S6 domain and facing the pore cavity of the channel is an important component of the binding site for a number of compounds[13,16]. To determine whether this key residue is also important for HERG channels blockade by ketanserin, we compared the inhibitory effects of ketanserin on WT and mutant (Y652A and Y652R) HERG channels. The effects of ketanserin on WT and Y652 mutant channels were quantified during a 2-s activating pulses to 0 mV from a holding potential of -80 mV, then the tail currents were evoked by repolarization to -70 mV. As shown in Fig. 5*A*, 10 μmol/L ketanserin significantly blocked the HERG channels. While Y652A mutant channels were partially blocked by 10 μmol/L ketanserin (Fig. 5*B*), and Y652R channel currents were approximately inhibited by ketanserin with similar concentration (Fig. 5*C*). WT HERG channels tail currents in oocytes were inhibited by ketanserin in a concentration-dependent manner with IC_{50} of (0.38±0.04) μmol/L at 0 mV. The IC_{50} for Y652A channel blockade at 0 mV was (27.13±9.40) μmol/L, 72-fold less sensitive than WT channel (Fig. 5*D*), while for Y652R, the value of IC_{50} was (20.20±2.80) μmol/L, 53-fold less sensitive than WT channel (Fig. 5*D*). And the inhibitory effects on Y652A and Y652R mutants had no marked distinction ($n=6$). These results indicated that Y652 mutant attenuated the blocking effect of ketanserin.

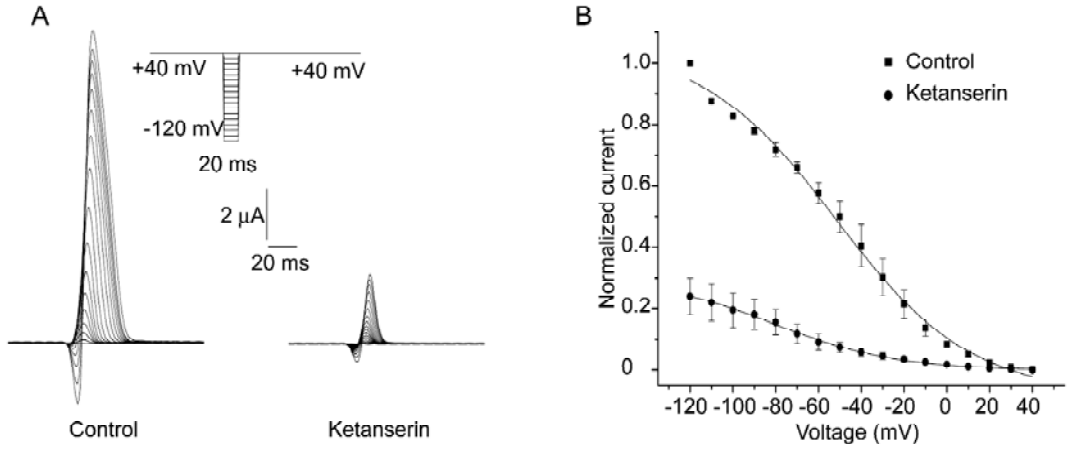

Fig. 4. Effect of ketanserin on wild-type HERG channel inactivation in *Xenopus* oocytes. *A*: Representative recording of the steady-state inactivation of HERG channels before (left) and after (right) incubation with 10 μmol/L ketanserin. After a 2-s pulse to +40 mV, the membrane potential was held to various test voltages from -120 mV to +40 mV for 20 ms to allow inactivation to relax to a steady-state, and then followed by a return step to +40 mV. *B*: Steady-state inactivation curves. Currents were elicited by a steady-state inactivation protocol in which inactivation was allowed to relax to steady-state during 20 ms test pulses to potential ranging from -120 to +40 mV. Peak currents were obtained from fitting the inactivating current with monoexponential equation and then plotted as a function of the preceding test pulse potentials. The inactivation curve was fitted with a Boltzmann function. Ketanserin shifted the voltage-dependent WT HERG channel inactivation curve from (-51.71±2.15) mV to (-80.76±14.98) mV ($P<0.05$, $n=4$). However, slope factors [(31.21±2.57) mV *vs* (28.82±9.69) mV)] for the steady-state inactivation were not significantly altered by ketanserin ($n=4$).

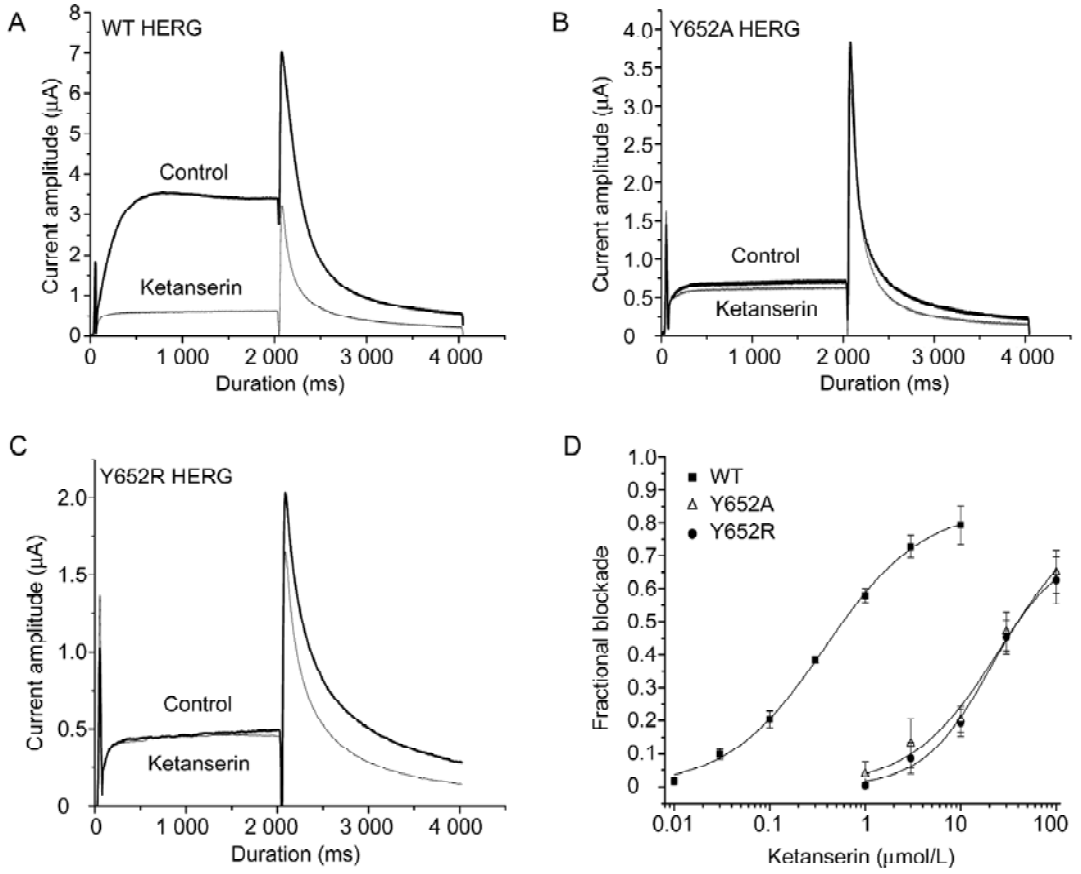

Fig. 5. Blockade of WT, Y652A and Y652R mutant HERG channels by ketanserin. *A*, *B* and *C*: Representative current records from cells expressing WT (*A*), Y652A (*B*) mutant and Y652R mutant (*C*) HERG channels elicited by the application of depolarization pulses to 0 mV, then repolarizing to -70 mV before and after exposure to 10 μmol/L ketanserin. *D*: Concentration-dependent blockade of HERG tail current by ketanserin at -70 mV. The IC_{50} value was (0.38±0.04) μmol/L, Hill coefficient was 0.85±0.05 for WT HERG, and IC_{50} was (27.13±9.40) μmol/L, Hill coefficient was 0.92±0.13 for Y652A mutant channel. The IC_{50} value was (20.20±2.80) μmol/L, Hill coefficient was 1.24±0.13 for Y652R HERG channel (n=6 for each group). The inhibitory effects on Y652A and Y652R had no marked distinction (n=6).

3 DISCUSSION

In clinical therapy, ketanserin can cause arrhythmia, which is considered as the result of the prolongation of APD and QT interval. The extension of APD could be due to ketanserin inhibiting multiple potassium currents in myocardial cells, e.g. I_{to}, I_{sus}, $I_{Kv1.3}$, I_{kr}, I_{ks} and so on, and these effects have no direct association with 5-$HT_{2A/2C}$ receptor[17,18]. Most drug-induced APD prolongation is mainly due to the inhibition of I_{kr} responsible for ventricular repolarization, although these drugs are structurally diverse[2]. It has been reported that ketanserin can prolong APD at concentrations from 0.1 to 10 μmol/L in clinical use[19,20]. Our present study showed that the IC_{50} value of ketanserin blocking HERG channel expressed in oocytes was (0.38±0.04) μmol/L, indicating that ketanserin could directly inhibit HERG channel to induce QT interval prolongation at therapeutic concentrations, and the blockade was concentration- and voltage-dependent, similar to rhynchophylline[21]. Our experiment with WT HERG channel suggested that ketanserin preferentially blocks open-state HERG channel, exhibiting several features that are typical of other open-channel blocker, such as dofetilide, chloroquine, ziparasidone and so on. First, there was no blockade of initial step current in response to depolarizing test pulse of -40 mV or more positive potentials. Meanwhile in the different depolarization duration, the fractional blockade of end-pulse step current and peak tail current at 100 ms duration was significantly lower than that at 400 ms and 700 ms duration, which indicates fractional blockade was enhanced by the channel activation. These data is consistent with an open-state channel blockade. Second, the extent

and rate of onset of blockade were voltage-dependent, and increased at more positive potentials even in the condition of leftward shift of activation curve, which increased the current amplitude at the test pulse negative to -40 mV and potentially enhanced current amplitude at other similar test potential positive to -40 mV. These results also suggested that channel activation is required by ketanserin blockade. Meanwhile, our research also showed ketanserin could modulate the inactivation of HERG channel.

To examine whether key molecular determinant of HERG channel blockade for previously investigated drugs are also important for HERG channels blockade by ketanserin, we compared the potency of channel blockade for WT and two mutant HERG channels (Y652A and Y652R). Y652 site is located on the S6 domain and faces the central cavity of the channel. The potency of channel blockade by ketanserin was dramatically reduced in two mutant HERG channels at equal concentration. Mutation of Y652A increased the IC_{50} by approximately 72-fold for HERG channel blockade, while mutation of Y652R increased the IC_{50} of ketanserin by 53-fold. As already stated, amino acids located on the S6 transmembrane domain (Y652) is demonstrated to be important in high-affinity blockade for a number of compounds[13,16,22-24]. Other voltage-gated K^+ channels (Kv1-Kv4) have Ile and Val (Ile) in the equivalent positions of the aromatic residues Y652 of HERG. In 2000, Mitcheson and colleagues showed that MK-499 interacted with the HERG channel, and that electrostatic interactions between π electrons and hydrogen atoms of the aromatic rings of Y652 and the drug molecule were crucial for high-affinity binding[25]. Similarly, in our study, for alanine-scanning mutagenesis of Y652, the potency of channel blockade by ketanserin was dramatically reduced. These results indicated that Tyr-652 is crucial for ketanserin-induced blockade of the HERG channel. Simultaneously, our research also demonstrated that using arginine to replace alanine located at Y652 site, the efficacy of channel blockade by ketanserin had no significantly difference, although their IC_{50} value was diverse.

In conclusion, the present study demonstrates that ketanserin preferentially binds to and blocks open-state HERG channels. Tyr-652 is one of critical molecular determinants for blockade of HERG channel by ketanserin.

* * *

ACKNOWLEDGMENTS: We thank Michael C. Sanguinetti for providing the cDNA of wide-type and mutant HERG channels and Guo He-Ping for technical and equipment supports.

REFERENCES

1 Warmke JW, Ganetzky B. A family of potassium channel genes related to eag in *Drosophila* and mammals. Proc Natl Acad Sci USA 1994; 91(8): 3438-3442.

2 Sanguinetti MC, Jiang C, Curran ME, Keating MT. A mechanistic link between an inherited and an acquired cardiac arrhythmia: HERG encodes the I_{Kr} potassium channel. Cell 1995; 81(2): 299-307.

3 Roden DM. Current status of class III antiarrhythmic drug therapy. Am J Cardiol 1993; 72(6): 44B-49B.

4 Cavero I, Mestre M, Guillon JM, Crumb W. Drugs that prolong QT interval as an unwanted effect: assessing their likelihood of inducing hazardous cardiac dysrhythmias. Exp Opin Pharmacother 2000; 1(5): 947-973.

5 De Ponti F, Poluzzi E, Cavalli A, Recanatini M, Montanaro N. Safety of non-antiarrhythmic drugs that prolong the QT interval or induce torsade de pointes. Drug Safety 2002; 25(4): 263-286.

6 January CT, Gong Q, Zhou Z. Long QT syndrome: cellular basis and arrhythmia mechanism in LQT2. J Cardiovasc Electrophysiol 2000; 11(12): 1413-1418.

7 Tseng GN. I_{Kr}: the hERG channel. J Mol Cell Cardiol 2001; 33(5): 835-849.

8 Mitcheson JS, Perry MD. Molecular determinants of high-affinity drug binding to hERG channels. Curr Opin Drug Discov Dev 2003; 6(5): 667-674.

9 van Schie DL, de Jeu DM, Stevn DW, Odendaal HJ, van Geijn HP. The optimal dosage of ketanserin for patients with severe hypertension in pregnancy. Eur J Obstet Gynecol Reprod Biol 2002; 102(2): 161-166.

10 Geerling RA, de Bruin RW, Scherinqa M, Bonthuis F, IJzermans JN, Marquet RL. Ketanserin reduces graft arteriosclerosis after allogeneic aorta transplantation in rats. J Cardiovasc Pharmacol 1996; 27(3): 307-311.

11 Arfiero S, Ometto R, Vincenzi M. Prolongation of the QT interval and torsade de pointes caused by ketanserin. G Ital Cardiol 1990; 20(9): 869-872.

12 Frishman WH, Huberfeld S, Okin S, Wang YH, Kumar A, Shareef B. Serotonin and serotonin antagonism in cardiovascular and non-cardiovascular disease. J Clin Pharmacol 1995; 35(6): 541-572.

13 Kamiya K, Niwa R, Mitcheson JS, Sanguinetti MC. Molecular determinants of HERG channel block. Mol Pharmacol 2006; 69 (5): 1709-1716.

14 Trudeau MC, Warmke JW, Ganetzky B, Robertson GA. HERG, a human inward rectifier in the voltage-gated potassium channel family. Science 1995; 269(5220): 92-95.

15 Milnes JT, Crociani O, Arcangeli A, Hancox JC, Witchel HJ. Blockade of HERG potassium currents by fluvoxamine: incomplete attenuation by S6 mutations at F656 or Y652. Br J Pharmacol 2003; 139(5): 887-898.

16 Mitcheson J, Perry M, Stansfeld P, Sanguinetti MC, Witchel H, Hancox J. Structural determinants for high-affinity block of hERG potassium channels. Novartis Found Symp 2005; 266: 136-150; discussion 150-158.

17 Le Grand B, Talmant JM, Rieu JP, Patoiseau JF, Colpaert FC, John GW. Investigation of the mechanism by which ketanserin prolongs the duration of the cardiac action potential. J Cardiovasc Pharmacol 1995; 26(5): 803-809.

18 Zhang ZH, Boutjdir M, el-Sherif N. Ketanserin inhibits depolarization-activated outward potassium current in rat ventricular myocytes. Circ Res 1994; 75(4): 711-721.

19 Knypl K, Wocial B, Berent H, Kuçzyńska K, Wasowska T, Brym E, Czerniewska E, Wacławek-Maczkowska J, Januszewicz W. Influence of chronic ketanserin therapy on blood pressure and certain humoral and metabolic factors in patients with mild to moderate primary essential hypertension. Pol Arch Med Wewn 1993; 90(2): 95-104.

20 Tekat D, Güler C, Arici M, Topalkara A, Erdoğan H. Effect of ketanserin administration on intraocular pressure. Ophthalmologica 2001; 215(6): 419-423.

21 Gui L, Li ZW, DU R, Yuan GH, Li W, Ren FX, Li J, Yang JG. Inhibitory effect of rhynchophylline on human *ether-a-go-go* related gene channel. Acta Physiol Sin (生理学报) 2005; 57(5): 648-652.

22 Duan JJ, Ma JH, Zhang PH, Wang XP, Zou AR, Tu DN. Verapamil blocks HERG channel by the helix residue Y652 and F656 in the S6 transmembrane domain. Acta Pharmacol Sin 2007; 28(7): 959-967.

23 Sãnchez-Chapula JA, Ferrer T, Navarro-Polanco RA, Sanguinetti MC. Voltage-dependent profile of human *ether-a-go-go*-related gene channel block is influenced by a single residue in the S6 transmembrane domain. Mol Pharmacol 2003; 63(5): 1051-1058.

24 Milnes JT, Crociani O, Arcangeli A, Hancox JC, Witchel HJ. Blockade of HERG potassium currents by fluvoxamine: incomplete attenuation by S6 mutations at F656 or Y652. Br J Pharmacol 2003; 139(5): 887-898.

25 Mitcheson JS, Chen J, Lin M, Culberson C, Sanguinetti MC. A structural basis for drug-induced long QT syndrome. Proc Natl Acad Sci USA 2000; 97: 12329-12333.